

GENERAL RADIO COMPANY
engineering department



REPRINT No. A93

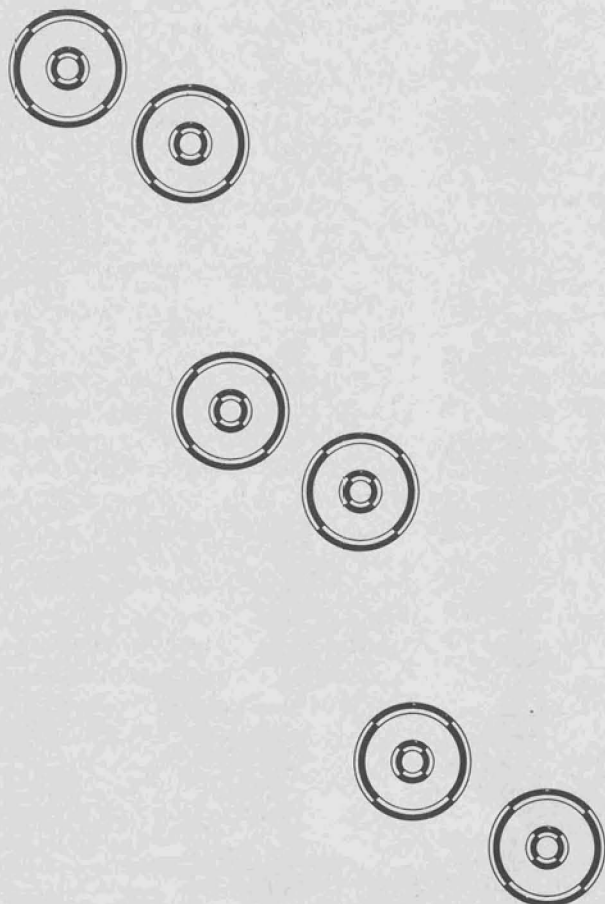
Reprinted from MICROWAVE JOURNAL

NOVEMBER, 1961

RF LEAKAGE CHARACTERISTICS
OF POPULAR COAXIAL CABLES
AND CONNECTORS, 500 MC TO 7.5 GC.

by

JOHN ZORZY
R. F. MUEHLBERGER



RF LEAKAGE CHARACTERISTICS OF POPULAR COAXIAL CABLES AND CONNECTORS, 500 MC TO 7.5 GC.

JOHN ZORZY
R. F. MUEHLBERGER

GENERAL RADIO COMPANY
West Concord • Massachusetts

Reprinted from THE MICROWAVE JOURNAL

November, 1961

Introduction

In the design and use of coaxial devices, a knowledge of the leakage characteristics of radio-frequency cables and connectors is important, both in measurements and in the design of operational and test equipment.

The evaluation and measurement of electromagnetic leakage through solid conductors, braids, screens, slits and other configurations employed to confine the electromagnetic fields in apparatus, has been the subject of a great deal of analysis and research. Some investigators have been concerned with the leakage phenomenon itself,^{1,2,3,4,5} others with its measurement^{6,7,8,9,10,11}. The experimental procedure employed is usually chosen in accordance with the particular manifestation of the electromagnetic leakage that is of interest. For example, for conducted leakage or coupling, a special direct metallic connection may be made between the leakage source and the detector; for induction or near-field leakage, probes or loops are placed in proximity with the leakage source; and, for radiated leakage, probes, loops, or the more distributed version of these, antennas, are placed at what is considered the far field of the leakage source. The three are commonly evaluated, *in toto*, by surrounding the leakage source with a closed coaxial system. The usual practice is to couple some of the basic leakage modes to the TEM mode of the coaxial system.

Usually the equipment designer is successful in confining stray electromagnetic fields within the equipment package except, of course, in open systems such as slotted lines. However, the connection of coaxial cables, flexible and solid, and coaxial components to the equipment introduces a source of leakage. In the case of immittance bridges, cable or connector leakage introduces a spurious signal path between the source and the detector, usually resulting in measurement errors. Leakage is a cause of error in precision slotted-line measurements through spurious coupling of the pick-up probe to the source; in attenuation measurements and filter-response measurements,

by spurious coupling between the input and the output circuits. In complex electronic systems, as for example in a missile system, the spurious coupling between the interconnecting cables of the separate systems can result in malfunction in the operation of an element of the system.

It is the purpose of this paper to demonstrate the relative shielding effectiveness of popular flexible cables and connectors, and to describe the measurement technique. Test results are presented in terms of both relative leakage power and surface transfer impedance. The unique feature of this work is the frequency range of measurement. The majority of previous contributions were concerned with the frequency range below 500 Mc.

Measurement Technique

The measurement of the leakage from connectors and cables is performed by collecting the leakage energy in a coaxial system surrounding the leakage source. An outline of the instrumentation is shown in Figures 1 and 2 respectively, and a photograph in Figure 3. The device from which leakage is to be measured, connector or cable, is incorporated in a uniform transmission line which is terminated in a matched load. The matched termination simplifies both the measurement procedure and data reduction. This complete coaxial system is embodied within a cylinder which forms, externally, a second coaxial system. The second coaxial system is terminated at one end in an adjustable short-circuiting plunger and at the other in a

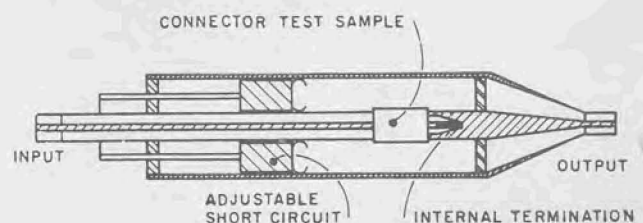


Figure 1 — Tri-Axial Connector Leakage Test Unit.

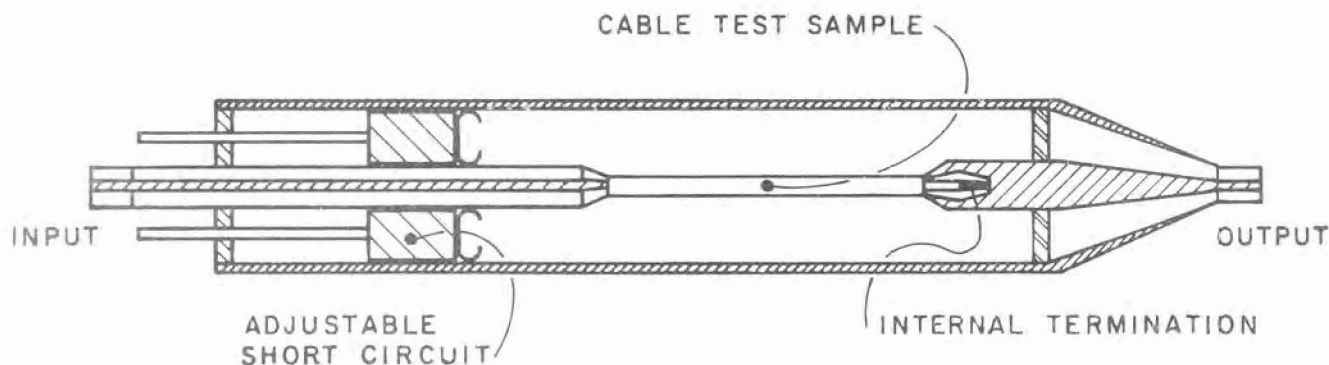


Figure 2—Tri-Axial Cable Leakage Test Unit.

tapered transition to a standard connector. In connector measurements, the outer coaxial line is terminated in a matched detector. Except for the adjustable short-circuit feature, this tri-axial system has been employed by others.^{6,7,8}

For direct leakage measurements the adjustable short circuit serves several purposes both in connector and cable measurements. In connector measurements, the short-circuit position is adjusted to assure that an adequately low impedance appears behind the equivalent leakage generator. A matched termination can be substituted, but the resulting 6-db loss cannot be tolerated in some cases. In addition, if the leakage source is directional, as it indeed is for cables and connectors with multiple leakage, it is possible for the leakage to be directed to this termination at some frequencies and not collected by the detector. For surface transfer-impedance measurements on cables or connectors with leakage from more than one point in the connector, however, a matched termination is desirable in order to simplify the transformation of the measured data to transfer impedance data. This latter consideration is discussed at greater length in the Appendix.

The equivalent leakage generator, in general, can have field components in the radial, axial, and circumferential*

directions. Furthermore, these components are not necessarily circularly symmetric. Locally, TE, TM, and TEM modes can all exist, and in fact, for complete leakage measurements, the detector should couple to all. The excitation of the outer coaxial line, however, is believed to be principally TEM, since the currents in the internal line are predominantly axial and symmetric. In the particular test configuration employed here, only the TE_{11} mode can be propagated, and this only above 3.5 Gc. In the transition to the smaller coaxial line, the TE_{11} mode is filtered out, but some of it couples to the principal TEM mode, delivering this power to the detector. Special care is taken to assure that the test cable or connector system is mounted concentrically, to minimize TE_{11} mode generation.

Despite the possible limitations cited above, the tri-axial system is a simple and effective system for measuring the net leakage. It is indeed well suited for axial surface transfer-impedance measurements. It can serve as a standard method only, however, if the leakage characteristics or axial surface transfer impedance of axially symmetrical components are to be evaluated. Accurate measurement of each mode of leakage, each manifestation of leakage, and each component of surface impedance will, in general, require a specific test configuration for the particular measurement.

The characteristic impedance of the outer coaxial line of the tri-axial system, which is formed with the cable

* The circumferential E-field component is not usually present in axially symmetric components. See References 1, 2.

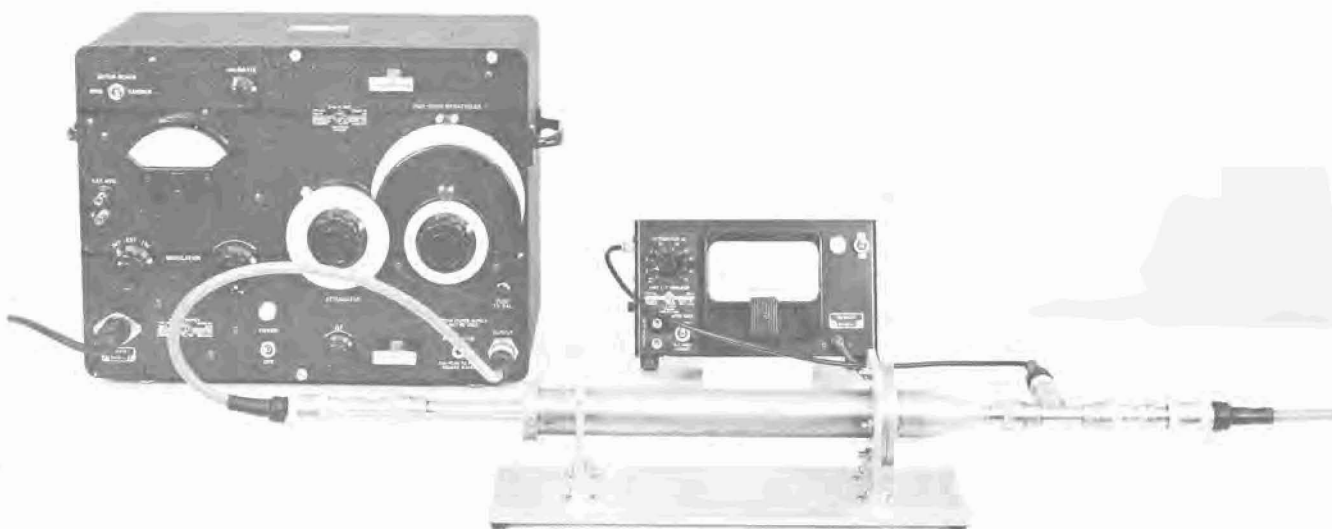


Figure 3—Tri-Axial Unit and Equipment Setup.

braid as the inner conductor, should be matched to the detector. As a matter of convenience, but with some sacrifice in accuracy and ease of data reduction, one outer conductor size was employed for all cables. The characteristic impedance was therefore generally higher than 50 ohms. The steps in conductor size at the cable connectors also produce capacitance discontinuities. These can be measured or calculated¹². The effects of the characteristic impedance discontinuity are described in the Appendix.

The leakage power ratio is defined here as the ratio of the power detected in a 50-ohm detector at the output of the tri-axial unit to the power flowing through the internal 50-ohm connector or cable system. It is basically the attenuation through the tri-axial system. This definition appears arbitrary in the sense that 50 ohms is an arbitrary load impedance. However, since the leakage source impedance is comparatively low, the voltage at the detector is essentially the open-circuit leakage voltage. The ratio of the input voltage to the leaky cable, to this output voltage is an absolute leakage quantity, as is the measured power ratio, which is identically equal to the square of this voltage ratio.

The surface transfer impedance is obtained from this ratio as follows:

The surface transfer impedance is,

$$Z_{21} = \frac{e_2}{i_1} \quad (1)$$

where

i_1 = Current flowing in internal line.

e_2 = Equivalent leakage voltage in external line.

In the connector leakage case, considering the equivalent leakage generator to be e_2 with an extremely low source impedance, this voltage e_2 appears at detector terminals, and the adjustable short circuit assures this. For a 50-ohm transmission-line system, the input power is,

$$50 i_1^2$$

The measured output power is,

$$\frac{e_2^2}{50}$$

The measured power ratio A^2 is therefore,

$$A^2 = \frac{\frac{e_2^2}{50}}{50 i_1^2} = \frac{e_2^2}{(50)^2 i_1^2} \quad (2)$$

Substituting and by definition,

$$Z_{21} = \frac{e_2}{i_1} = 50 A \quad (3)$$

In the cable leakage case, the calculation is not as straightforward, especially where the outer tri-axial line is not terminated in its characteristic impedance. The calculations required to reduce the measured results given in this paper to transfer impedance per unit length are not included for that reason. The tri-axial system was set up principally to assess the relative leakage.

For the measurement of surface transfer impedance of cables, the outer coaxial line of the tri-axial system should be terminated in its characteristic impedance at the source end and in a similarly matched detector at the output end. In this case the relation between the measured leakage power ratio, A^2 , and the surface transfer impedance per unit length is, in a 50-ohm system,

$$Z_{21} = \frac{100 A (\beta - \beta_0)}{1 - e^{-j(\beta - \beta_0)L}} \quad (4)$$

where

L = length of leaky cable section.

β = propagation constant in the test cable.

β_0 = propagation constant in external line of tri-axial system.

This expression is obtained from Equation (5) in the Appendix which describes the forward TEM wave launched by the cable.

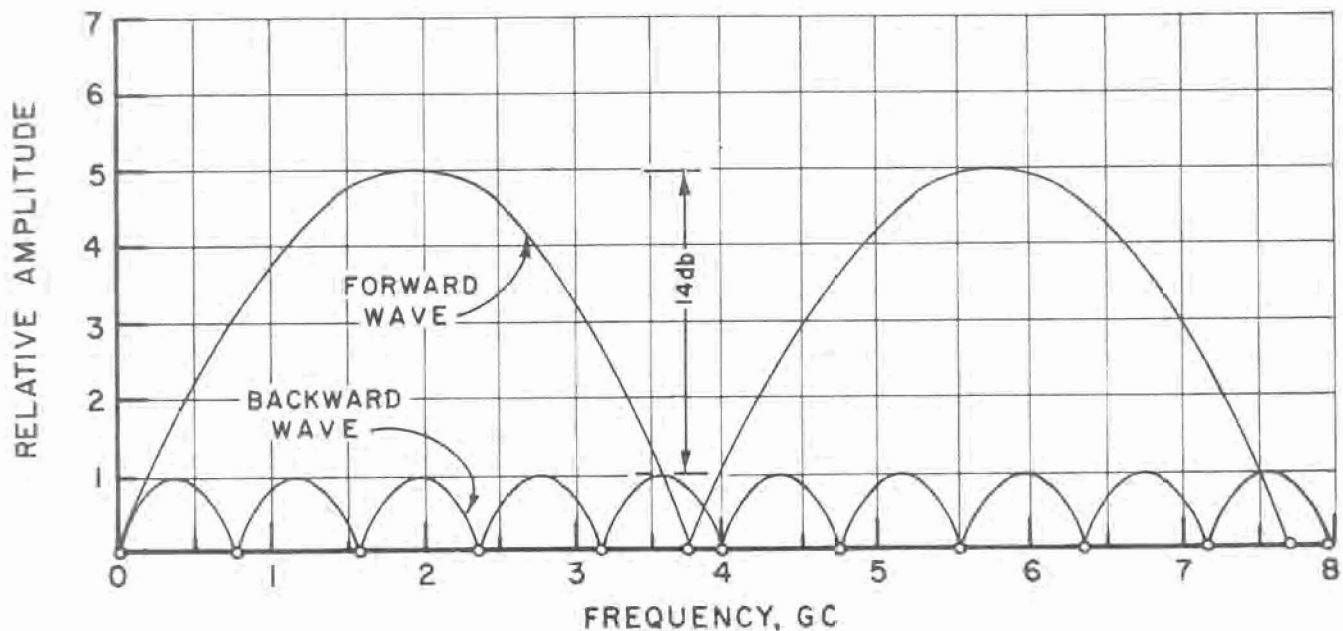


Figure 4 — Forward and Backward Wave, Matched Case, $\frac{\beta - \beta_0}{\beta_0} = 0.52$, 15-cm Long Cable.

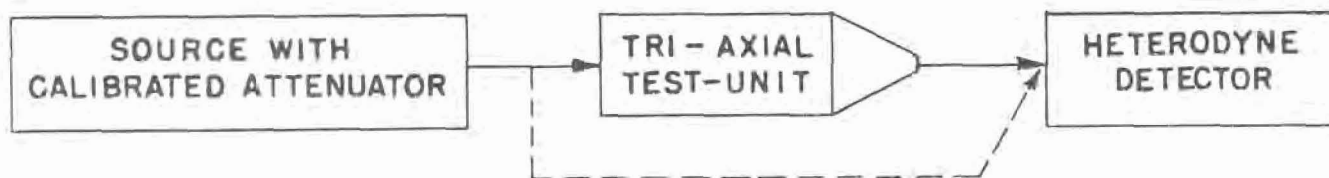


Figure 5 — Block Diagram of the Measuring System.

A null in this forward wave occurs when $(\beta - \beta_0)L = 2n\pi$ and a maximum when $(\beta - \beta_0)L = (2n - 1)\pi$. The variation of forward wave amplitude with frequency is shown in Figure 4. Also shown is the backward wave, which is the signal that would appear in a detector at the source end of the outer line. This is obtained from Equations (5) and (9) in the Appendix, employing a polyethylene-dielectric internal line and air-dielectric external line.

Measurement Procedure

In measuring the leakage power ratio, A^2 , basically a substitution technique is employed. A matched detector system is installed at the output connector of the tri-axial unit, and the unit is driven as shown in Figure 5. In this setup, the short circuit is adjusted to produce a maximum indication at the detector. The detector is then connected directly to the source through a calibrated attenuator, and the attenuation required to yield the initial detector level is measured.

The sensitivity of this system is obviously limited by the sensitivity of the detector and the power available. A sensitive superheterodyne system was employed, and for the low-leakage configurations about 30 milliwatts of power was required.

The principal sources of error are attenuator errors and mismatch at the receiver (mixer) input. For connector measurements, the error due to mismatch is directly proportional to VSWR since the equivalent leakage source impedance is small. The indicated leakage power can vary between the extremes, $P \times \text{VSWR}$ to $P \div \text{VSWR}$, where P is the power that would be delivered to a matched system. A VSWR of 2 will produce ± 3 -db error therefore.

In advance of installing the inner coaxial system into the outer cylinder of the tri-axial system, the inner system may be excited, and the immediate vicinity of the leakage point or associated connector and attachment points probed with a small loop or dipole to establish how critical are the mating of the connector and cable joints.

Test Results

Connector Leakage and Surface Transfer Impedance

The above procedure was employed to assess the leakage characteristics of three widely used connectors, the General Radio 874-B, the BNC (Bayonet Coupling), and the N (Threaded Coupling), and in addition, the new General Radio Locking Connector, the 874-BL which comprises the basic 874-B Connector with an outer, threaded coupling nut to shield and join the mating parts securely.

Leakage results are shown in Figure 6. These results were transformed to equivalent transfer impedance, Z_{21} , and this result is shown in Figures 7 and 8.

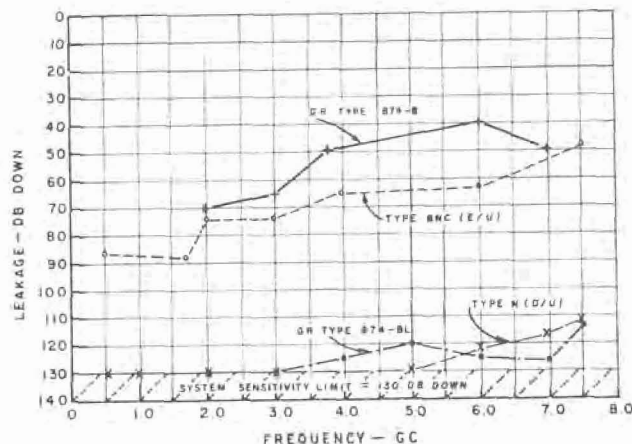


Figure 6 — Leakage Characteristics of the Type BNC, N, and General Radio Type 874-B, and Type 874-BL Connectors.

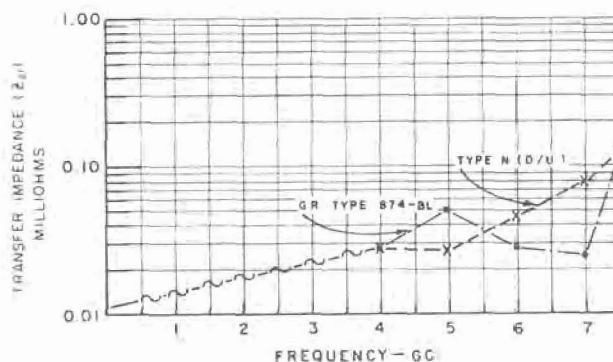


Figure 7 — Surface Transfer Impedance of the Type N and General Radio Type 874-BL Coaxial Connectors.

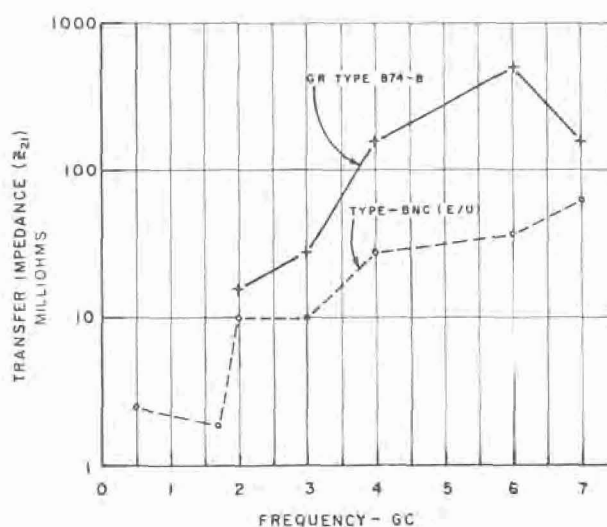


Figure 8 — Surface Transfer Impedance of the Type BNC and General Radio Type 874-B Coaxial Connectors.

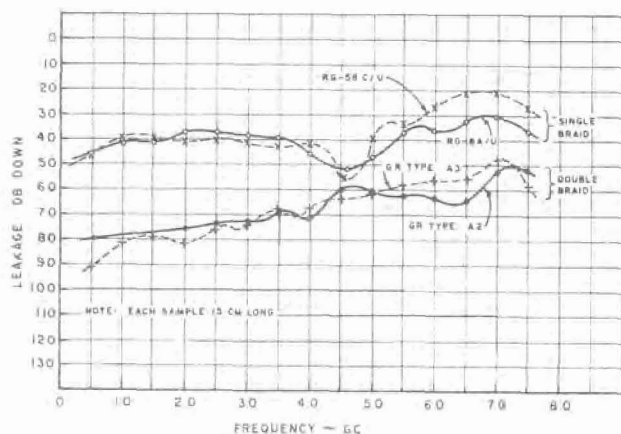


Figure 9—Leakage Characteristics of RG-58, RG-8, and General Radio Types 874-A2 and 874-A3 Flexible Coaxial Cables.

The leakage characteristics of several popular flexible coaxial cables are shown in Figure 9. The RG-8 and RG-58 are single-braid cables. The General Radio A-2 and A-3 are double-braid cables of approximately the same size as RG-8 and RG-58 respectively. The corresponding surface impedance per unit length, calculated from the leakage measurements, is shown in Figures 10 and 11. Simple theory indicates that the transfer impedance is principally inductance. A linear surface impedance variation with frequency is, therefore, predicted. A linear frequency curve is shown in the graphs in this connection. For single-braid cables, the linear relation exists up to about 5 Gc, while for the double-braid cables the linear relation exists only up to about 2 Gc.

The single-braid leakage data indicate the periodicity expected in the forward wave launched by the leaky cable, and is explained, therefore, by an orderly arrangement of incremental leakage sources.

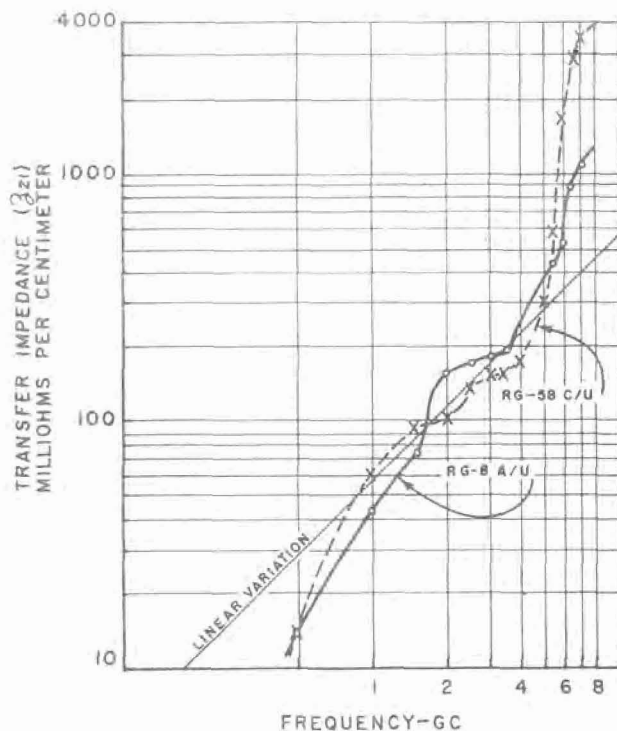


Figure 10—Surface Transfer Impedance Per Unit Length of RG-58 and RG-8 Single-Braid Cables.

The double-braid data are devoid of the periodic variation. Perhaps the double-shield arrangement cannot be represented as a series of equal incremental generators as well as can the single-braid, because the contact between the outer and inner braids may not be as regular as the weave of the braid. Subsequent measurements will be performed to verify this result, and to separate the forward and backward waves launched by the cable. This will permit a more accurate measurement of transfer impedance.

APPENDIX

The Forward and Backward Waves Launched by Leaky Cables—Analysis

Loose coupling between adjacent transmission lines under matched conditions has been analyzed typically by Shelkunoff and Odarenko¹³, and Jungfer¹⁴. An analysis is given here for the coupling of the leaky cable into the secondary, external coaxial line of the tri-axial system, under general conditions of match. The particular case in which the source end of the external, collecting line is terminated in a short-circuit, and the output end of the external line is terminated in a load not matched to this line, is also analyzed.

Voltage at Output End and Forward Wave

The wave propagating toward the output is given as the forward wave. It is the signal appearing at a detector

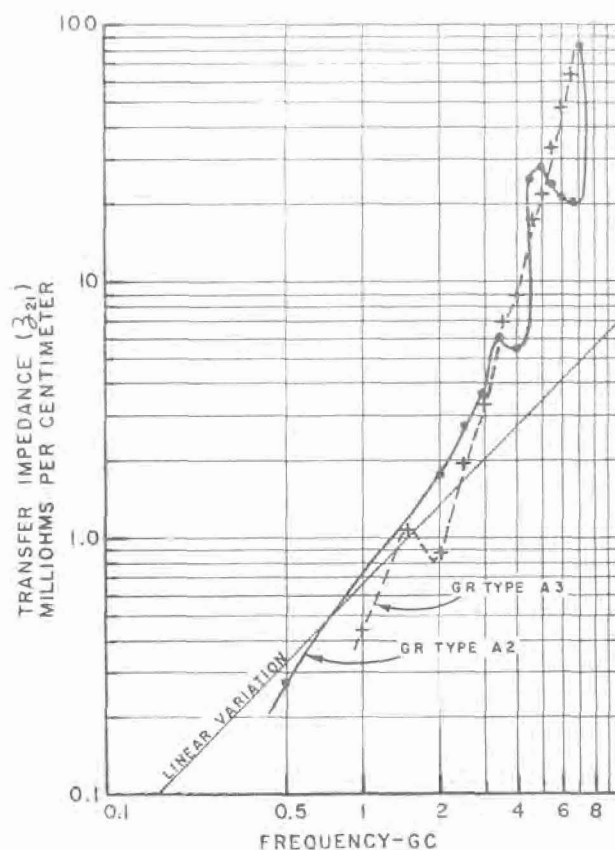


Figure 11—Surface Transfer Impedance Per Unit Length of General Radio Types 874-A2 and 874-A3 Flexible Coaxial Double-Braid Cables.

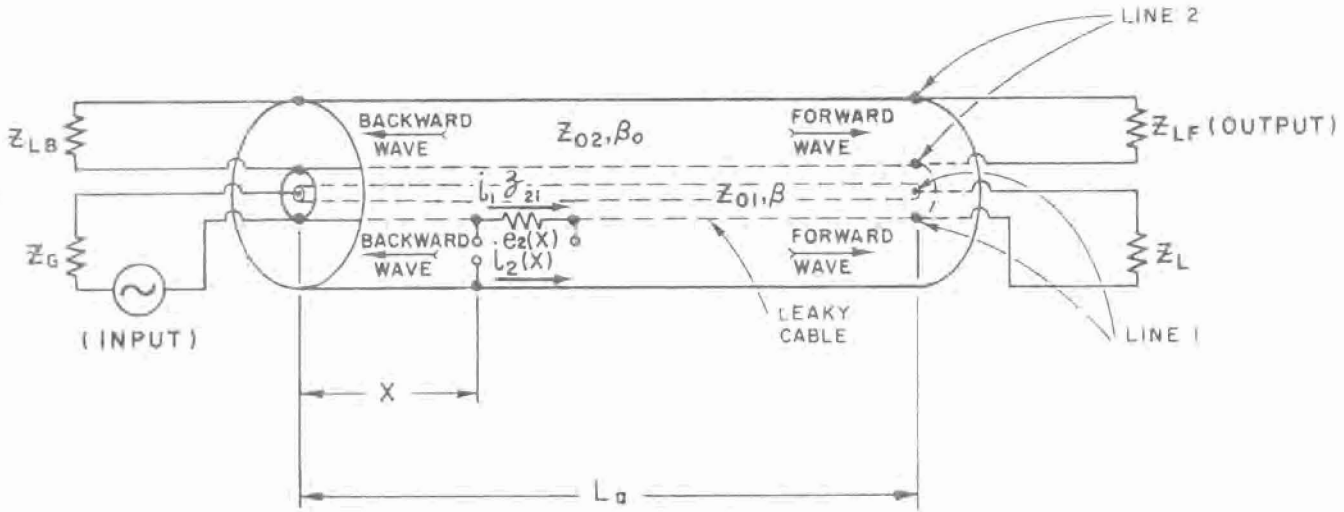


Figure 12 — Schematic, Tri-Axial Transmission System.

placed at the output end of the tri-axial unit under matched conditions. The total voltage at the output end is obtained as follows:

In Figure 12, current, i_1 , flowing internally in the cable produces the voltage e_2 at the surface impedance, z_{21} . This voltage appears externally in series with the cable outer conductor and produces a current $i_2(x)$, in the outer line.

The wave to the right produced by $i_2(x)$ is obtained as follows:

The incremental voltage e_2 at x is

$$e_2(x) = i_1 z_{21} e^{-j\beta x} dx \quad (1)$$

where: i_1 = current in internal line (assumed uniform),

z_{21} = surface transfer impedance per unit length.

β = propagation constant in cable.

The incremental current in the external line 2, at plane x is therefore,

$$\begin{aligned} i_2(x) &= \frac{e_2(x)}{Z_2(x)} \\ &= \frac{i_1 z_{21}}{Z_2(x)} e^{-j\beta x} dx \end{aligned} \quad (2)$$

where:

$Z_2(x)$ = the series combination of Z_{LF} , transformed to plane x , and Z_{LB} transformed to plane x ,
 $= Z_B(x) + Z_F(x)$.

$$Z_B(x) = Z_{02} \frac{Z_{LB} + j Z_{02} \tan \beta_0 x}{Z_{02} + j Z_{LB} \tan \beta_0 x}$$

$$Z_F(x) = Z_{02} \frac{Z_{LF} + j Z_{02} \tan [\beta_0 (L_0 - x)]}{Z_{02} + j Z_{LF} \tan [\beta_0 (L_0 - x)]}$$

L_0 = length of leaky cable.

β_0 = propagation constant in external line.

The incremental voltage across the external line at $x = L_0$, or across Z_{LF} is,

$$\begin{aligned} de_F &= [e_2(x) - i_2(x) Z_B(x)] \cos [\beta_0 (L_0 - x)] \\ &\quad - j [i_2(x) Z_{02}] \sin [\beta_0 (L_0 - x)] \\ &= i_1 z_{21} \left[1 - \frac{Z_B(x)}{Z_2(x)} \right] \cos [\beta_0 (L_0 - x)] e^{-j\beta x} dx \\ &\quad - j i_1 z_{21} \left[\frac{Z_{02}}{Z_2(x)} \right] \sin [\beta_0 (L_0 - x)] e^{-j\beta x} dx \end{aligned} \quad (3)$$

Integration of (3), which is the summation of the contributions from the series of incremental leakage generators, yields the total voltage across Z_{LF} , that is,

$$\begin{aligned} e_F(L_0) &= i_1 z_{21} \int_0^{L_0} \left\{ \left[1 - \frac{Z_B(x)}{Z_2(x)} \right] \cos [\beta_0 (L_0 - x)] e^{-j\beta x} \right. \\ &\quad \left. - j \left[\frac{Z_{02}}{Z_2(x)} \right] \sin [\beta_0 (L_0 - x)] e^{-j\beta x} \right\} dx \end{aligned} \quad (4)$$

Note that when the external system is matched at both ends, (4) reduces to the forward wave:

$$e_F(L_0) = j \frac{i_1 z_{21}}{2(\beta - \beta_0)} e^{-j\beta_0 L_0} \left[1 - e^{-j(\beta - \beta_0)L_0} \right] \quad (5)$$

For the tri-axial connections described in the text, the output voltage was the sum of the complex voltages of the forward and backward waves obtained by integration of Equation (4).

For this setup, Z_{LB} was a short-circuited length of coaxial line of characteristic impedance Z_{03} . In this case,

$$Z_{LB} = j Z_{03} \tan (\beta_0 L_0)$$

In addition, the load Z_{LF} was not matched to Z_{02} , therefore, Equation (4) applies, employing the above substitution for Z_{LB} in $Z_B(x)$, wherein $Z_2(x) = Z_B(x) + Z_F(x)$.

In the experimental procedure, L_0 , the length of the short circuit is adjusted to produce a maximum in the total voltage across Z_{LF} , the detector impedance. The result of integration of (4) for this general case is complex.

Therefore, in order to illustrate the summation of the forward and backward wave, when a short circuit is used, consider the case where the external line is terminated in a matched detector at the output end, and $Z_{03}=Z_{02}$. The total voltage across Z_{L1} , simplifies to,

$$e_F = \frac{i_1 z_{21}}{2} \left[\frac{1 - e^{-j(\beta - \beta_0)L_a}}{\beta - \beta_0} + \frac{1 - e^{-j(\beta + \beta_0)L_a}}{\beta + \beta_0} e^{-j\beta L_1} \right] \quad (6)$$

When the short circuit is adjusted for maximum output voltage this reduces to,

$$e_F(\max) = \frac{i_1 z_{21}}{2} \left[\left| \frac{1 - e^{-j(\beta - \beta_0)L_a}}{\beta - \beta_0} \right| + \left| \frac{1 - e^{-j(\beta + \beta_0)L_a}}{\beta + \beta_0} \right| \right] \quad (7)$$

The first term is recognized as the forward wave for the matched case, Equation (5). The second term is recognized as the backward wave for the matched case, Equation (9) below.

Voltage at Input End and Backward Wave

The wave propagating toward the source or input is given as the backward wave. It is the signal appearing at a detector placed at the input end of the tri-axial unit under matched conditions. The total voltage at the input end is obtained in the same manner as for the forward wave, yielding the following result:

$$e_B(0) = i_1 z_{21} \int_0^{L_a} \left\{ \left[1 - \frac{Z_F(x)}{Z_2(x)} \right] \cos(\beta_0 x) e^{-j\beta x} - j \left[\frac{Z_{02}}{Z_2(x)} \right] \sin(\beta_0 x) e^{-j\beta x} \right\} dx \quad (8)$$

This is the total voltage across Z_{L1} .

Note that when the external system is matched at both

ends, (8) reduces to the backward wave:

$$e_B = j \frac{i_1 z_{21}}{2(\beta + \beta_0)} \left[1 - e^{-j(\beta + \beta_0)L_a} \right] \quad (9)$$

These equations describe the frequency behavior of the tri-axial unit leakage output voltage, and relate this to the surface transfer impedance. The measured result is the ratio of power at output to power input incident on internal cable, and is directly related to e_F/i_1 . The transfer impedance, z_{21} , is calculated from this measured result, employing the value for L_a obtained by physical measurement and from known or measured values of the propagation constants β and β_0 .

References

1. K. Ikrath, "Leakage of Electromagnetic Energy from Coaxial Cable Structures," Proc. of the Fourth Conf. on Radio Interference Reduction and Electronic Compatibility, pp. 311-357, Oct. 1-2, 1958.
2. D. P. Kanellakos and L. C. Peach, "The Performance of Shielding Materials," Proc. of the Fifth Conf. on Radio Interference Reduction and Electronic Compatibility, pp. 316-341, Oct. 6, 7, 8, 1959.
3. J. D. Meindl and E. R. Schatz, "The External Electromagnetic Fields of Shielded Transmission Lines," Proc. of the Sixth Conf. on Radio Interference Reduction and Electronic Compatibility, pp. 388-405, Oct. 4, 5, 6, 1960.
4. H. Kaden, Wirbelströme und Schirmung in der Nachrichtentechnik, Springer-Verlag, Berlin, pp. 272-282, (1959).
5. L. Krügel, Abschirmwirkung Von Aussenleitern Flexibler Koaxialkabel, Telefunken-Zeitung, Jg 29, pp. 256-266, Dec., 1956, heft 114.
6. H. Jungfer, "Die Messung des Kopplungswiderstandes Von Kabelabschirmungen bei hohen Frequenzen," NTZ, Jg 9, pp. 553-560, Aug. 1956, heft 8.
7. J. A. Allen, "A Proposed Standard for Testing the Shielding Effectiveness of Coaxial Cables and Shielding Materials," Proc. of the Sixth Conf. on Radio Interference Reduction and Electronic Compatibility, pp. 372-387, Oct. 4, 5, 6, 1960.
8. Handbook of Microwave Measurements, Vol. I, Polytechnic Inst. of Brooklyn, M. R. L. (1954), Section XI.
9. R. F. Robl and E. R. Schatz, "A Free-Space Method for Measuring Coaxial Cable Shielding Effectiveness," Proc. of the Fourth Conf. on Radio Interference Reduction and Electronic Compatibility, pp. 372-386, Oct. 1, 2, 1958.
10. A. R. Anderson, "Cylindrical Shielding and its Measurement at Radio Frequencies," Proc. IRE, 34, 5, pp. 312-322, May, 1946.
11. L. Krügel, "Mehrfachschirmung Flexibler Koaxial Kabel," Telefunken-Zeitung, Jg 30, pp. 207-214, September, 1957, heft 117.
12. T. Moreno, Microwave Transmission Design Data, 1st Ed., McGraw-Hill Book Co., Inc., New York, p. 96, (1948).
13. S. A. Shelkunoff and T. M. Odarenko, "Crosstalk Between Coaxial Transmission Lines," Bell Sys. Tech. J., Vol. XVI, No. 2, pp. 144-164, April, 1937.
- a.) K. E. Gould, "Crosstalk in Coaxial Cables — Analysis Based on Short-Circuited and Open Tertiaries," Bell Sys. Tech. J. 19, 341, (1940).
- b.) R. P. Booth and T. M. Odarenko, "Crosstalk Between Coaxial Conductors in Cable," Bell Sys. Tech. J., 19, 358, (1940).
- c.) S. A. Shelkunoff, "Electromagnetic Waves," D. Van Nostrand Inc., Princeton, N.J., (1943). (See page 228, Surface Transfer Impedance).
- d.) C. G. Montgomery, "Technique of Microwave Measurement," 1st Ed. (1947) McGraw-Hill Book Co., Inc., New York, (1947).

GENERAL RADIO COMPANY

* WEST CONCORD, MASSACHUSETTS

*NEW YORK: Broad Avenue at Linden
Ridgefield, New Jersey

SYRACUSE: Pickard Building, East Molloy Road
Syracuse 11, New York

PHILADELPHIA: 1150 York Road
Abington, Pennsylvania

SAN FRANCISCO: 1186 Los Altos Avenue
Los Altos, California

*WASHINGTON: Rockville Pike at Wall Lane
Rockville, Maryland

CLEVELAND: 5579 Pearl Road
Cleveland 29, Ohio

*CHICAGO: 6605 West North Avenue
Oak Park, Illinois

*TORONTO: 99 Floral Parkway
Toronto 15, Ontario

FLORIDA: 113 East Colonial Drive
Orlando, Florida

DALLAS: 2501-A West Mockingbird Lane
Dallas 35, Texas

*LOS ANGELES: 1000 North Seward Street
Los Angeles 38, California

MONTREAL: Office 395 1255 Laird Boulevard
Town of Mount Royal, Quebec, Canada

*Repair services are available at these offices.

GENERAL RADIO COMPANY (Overseas), Zurich, Switzerland
Representatives in Principal Overseas Countries

Printed in U.S.A.